Numerical study of turbulent characteristics over rough bed

[1]Sayahnya Roy, [2]Abhishek Chattrjee, [3]Koustuv Debnath

Department of Aerospace Engineering & Applied Mechanics
BENGAL ENGINEERING AND SCIENCE UNIVERSITY, Howrah, WB
Email : [1]Sayahnya1110@gmail.com, [2]abhishek.chatt@yahoo.com, [3]debnath_koustuv@yahoo.com

Abstract- The paper covers the k - ε turbulence model for numerical studying only current flow over cubic and pyramid shaped roughness. It mainly focuses on the turbulent characteristics over those two type of roughness for flow having Reynolds number 40,000 and 60,000. The comparison of vertical distribution of the mean velocity, turbulent intensity, and turbulent kinetic energy between the two types of roughness at tops and troughs is explored.

Keywords- Turbulence, cubic and pyramid shape roughness, K-epsilon model.

I. INTRODUCTION

Most of the environmental flows are hydraulically rough. Generally the roughness elements above the bed surface are located in between the viscous sub layer and the turbulent region. Due to their existence and complexity, turbulent flow over rough surface have been studied in past by numerous researchers (e.g. Leonardi et al. 2003, Jimenez. 2004, Stoesser and Rodi. 2004). The traditional approach to study rough beds open channel flows are based on time averaged hydrodynamic equation as Reynolds averaged navier-stokes equation, which is very convenient for modelling and describing the numerical results. K-epsilon turbulent model is also based on this hydrodynamic equation. Several experiments and numerical simulations (e.g. Jorge bailon-cuba at el. 2009, Thorsten stoesser and Vladimir I.Nikora. 2008, A.Keshmiri. 2012 etc.) has been carried out on the turbulent characteristics over different geometry. From all the papers it may be concluded that those simulations are not much focused on the comparative study over cubic and pyramid shape roughness for different Reynolds number. Therefore the main objective of the present paper is to describe the numerical simulations performed with the aim of studying the effect of different geometry on the turbulent characteristics for different Reynolds number. The motivation of the study is to compare the turbulent kinetic energy, the turbulent intensity and stream wise mean velocity profile between cubic and pyramid roughness for different Reynolds number.

II. RANS MODELLING

The fluid flow equations that are solved to characterize the flow structure in vegetated channels are the Reynolds-averaged Navier-Stokes (RANS) equations given in tensor notation by

$$\frac{\partial \overline{u_i}}{\partial x_i} = o \qquad (1)$$

$$\frac{\partial \overline{u_i}}{\partial t} + \frac{\partial}{\partial x_j}(\overline{u_j}\,\overline{u_i}) = -\frac{\partial \overline{p}}{\partial x_i} + \nu \frac{\partial^2 \overline{u_i}}{\partial x^2{}_j} - \frac{\partial}{\partial x_i}(\overline{u_i{}' u_j{}'}) \qquad (2)$$

where the Reynolds averaged quantity is denoted by over bar. Here, $\overline{u_i}$ and $u_i{}'$ denotes mean and fluctuating velocities in the x_i direction, respectively with i = I, 2, or 3 representing the stream-wise x, span-wise y, or vertical z directions; x_i = (x, y, z) $^{\Omega}$ x; u_i= (u, v, w); $\overline{u_i}$= (u, v, w) $^{\Omega}$ (U, V, W); n= kinematic viscosity; and p =kinematic pressure. Reynolds-averaging the Navier-Stokes equation gives rise to unknown correlations between the fluctuating velocities called Reynolds stresses defined by the tensor $\overline{u_i{}' u_j{}'}$. Physically these correlations, multiplied by density (r), i.e., p $\overline{u_i{}' u_j{}'}$ is the transport of\ momentum in the direction of x_j Eqs. (1) and (2) can be solved for the mean values of velocity, pressure, etc., when these turbulent correlations can be related with mean velocity or pressure. This is called the closure problem of turbulence modelling. Boussinesq's eddy-viscosity concept was used here to model the Reynolds stress given by

$$-\overline{u_i{}'u_j{}'} = v_t\left(\frac{\partial \overline{u_i}}{\partial x_j}+\frac{\partial \overline{u_j}}{\partial x_i}\right)-\frac{2}{3}\kappa\delta_{ij} \quad (3)$$

where v_t= turbulent or eddy viscosity, that depends on the state of turbulence and may vary from one point in the flow to another; k = 0.5 $\overline{u_i{}'u_j{}'}$ is the turbulent kinetic energy (TKE); and δ_{ij}= the Knonecker detla function. The eddy viscosity is again unknown but dimensional analysis indicated that

$$v_t = C_\mu(\kappa^2/\varepsilon \quad (4)$$

where ε = rate at which TKE is converted into thermal internal energy; C_μ = closure coefficient = 0.09. The modelled transport equation for k and ε called the k- ε two equation turbulence model (Launder and Spalding 1972) is used here in conjunction with Eqs. (1)- (4) to form a closed set given by

$$\frac{\partial \kappa}{\partial t}+\frac{(\partial \overline{u_j}\kappa)}{\partial x_j}=\frac{\partial}{\partial x_j}\left[\left(v+\frac{v_t}{\sigma_\kappa}\right)\frac{(\partial \kappa)}{\partial x_j}\right]+P-\varepsilon \quad (5)$$

$$\frac{\partial \varepsilon}{\partial t}+\frac{(\partial \overline{u_j}\varepsilon)}{\partial x_j}=\frac{\partial}{\partial x_j}\left[\left(v+\frac{v_t}{\sigma_\varepsilon}\right)\frac{(\partial \varepsilon)}{\partial x_j}\right]+\frac{\varepsilon}{\kappa}(C_{\varepsilon 1}P-C_{\varepsilon 2}\varepsilon \quad (6)$$

Where P= $\overline{u_i{}'u_j{}'}(\partial \overline{u_i}/\partial x_j)$is the production of k; σ_κ= 1.0 (turbulence Prandtl number for k); σ_ε = 1.3 (turbulence Prandtl number for ϵ); and $C_{\varepsilon 1}$= 1.44, $C_{\varepsilon 2}$= 1.94 are constants for the ϵ equation.

III. VOF MODEL OF AIR-WATER TWO PHASE FLOW OF OPEN CHANNEL

Volume of fluid (VOF) originally proposed by Hirt and Nichols (1981) was used in generation of the rough bed open channel model with free surface. The VOF method can model two or more immiscible fluids by solving a single set of momentum equations and tracking the volume fraction of each of the fluids throughout the domain. The basic concept of this type of model is that the two fluids are not interpenetrating. Using two fluids in this problem introduce a new variable i.e., the volume fraction of the phase in the computational cell. Therefore, as for air and water flow field, a single set of momentum equation shared by air and water, and the volume fraction of each of the fluid in each computational cell is tracked throughout the domain. In each computational cell, the volume fractions of all phases sum to unity. The fields for all variables and properties are shared by the phases and represent volume-averaged values, as long as the volume fraction of each of the phases is known at each location. Thus the variables and properties in any given cell are either purely representative of one of the phases, or representative of a mixture of the phases, depending upon the volume fraction values. In other words, if the q_{th} fluid's volume fraction in the cell is denoted as α_q, then the following three conditions are possible: (a) α_q = 0, when the cell does not contain the q_{th} fluid, indicating that the cell is full of air for water-air problem; (b) α_q = 1 when the q_{th} fluid occupies the entire cell indicating that the cell is full of water for water-air problem; and (c) 0 < α_q < 1 when the cell contains the interface between the q_{th} fluid and one or more other fluids, i.e., for air water interface this will correspond to a free surface. If α_w= volume fraction of water and α_a = volume fraction of water, the tracking of interface between air and water is accomplished by the solution of the continuity equation given by

$$\frac{\partial \alpha_w}{\partial t}+\overline{u_i}\frac{\partial \alpha_w}{\partial x_i}=0 \quad (7)$$

VOF implicit scheme is used to determine the detailed location of the free surface i.e., the interface between air and water has a linear slope within each cell and uses this linear shape for calculation of advection of fluid through the corresponding cell face. Thus with the volume fraction value and its derivatives in the cell, the position of the linear interface relative to the centre of each partially filled cell is evaluated. In the VOF model, because water and air phases share same velocity and pressure field, single set of equations can describe the flow field of air-water two-phase flow similar to a single-phase flow. Therefore, after creation of the VOF model, the k - ε turbulence model is a homogeneous flow model of two-phase flow. The equations of k - ε turbulence model with the VOF method are given by Eqs. (1) - (6) except for the expressions for density p and molecular viscosityμ , which are the volume fraction averaged properties. They are functions of water content α_w, and are not constants. They can be determined by the content of air and water in each cell as below (Chen et al. 2002):

$$\rho = \alpha_w\rho_w + (1-\alpha_w)\rho_a \quad (8)$$

$$v = \alpha_w v_w + (1-\alpha_w)v_a \quad (9)$$

where ρ_w and ρ_a = density of water and air; and v_w and v_a = kinematic viscosity of water and air, respectively. By iterating the solution of volume fraction of water α_w, ρ and v can be calculated. In Eqs. (1-6) there are six unknown variables, i.e., $\overline{u_i}$ (I= 1, 2, 3), $\bar{p}$, k and ε. With the VOF model Eq. (7) is solved in addition to Eqs. (1)-(6) and the 6 unknown variables in addition to α_w is solved.

IV. DOMAIN DESCRIPTION OF THE OPEN CHANNEL MODEL AND BOUNDARY CONDITIONS

Un-staggered scheme is used to mesh of the open channel of rectangular cross section with roughness. The open channel is taken to be of rectangular cross-section with constant height 0.8 m and total length 18 m. The air portion is kept of total depth 0.4 m, large enough to

avoid any effect from the boundary condition at the top of the domain. Salaheldin et al. (2004) reported that if air depth to water depth is kept more than

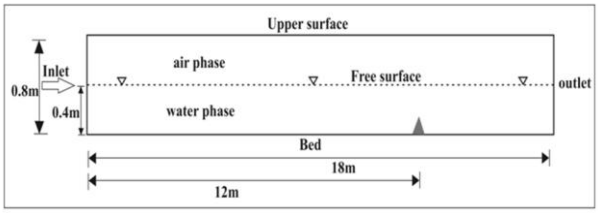

Fig.1 layout of channel model for numerical simulation

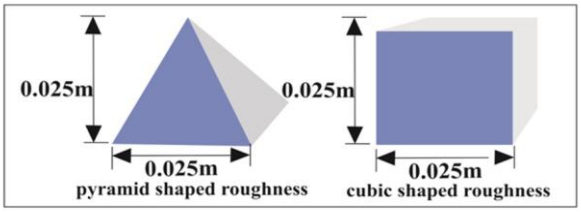

0.5 there is no effect from the boundary at the top. The roughness portion of the channel is meshed using a maximum edge length of 0.005 m and the flow developing region upstream of the roughness region is meshed using a maximum edge length of 0.1 m along the channel length and 0.03 m along channel height for all the models constructed. We have tested several schemes of discretization of the rough bed channel models, however, use of any other scheme resulted in (e.g., mapped meshing, tetrahedral primitive) large number of distorted elements with high values of skewness and often resulted in negative volumes. However, with use of un-staggered scheme with hexahedral elements, we achieved convergence with reasonable computational effort.

Boundary conditions were applied to simulate our present study by using two separate inlets for air and water and uniform distributions were given for all the dependant variables. Different boundary conditions used from FLUENT14 drop down menu on boundary conditions for different faces of the open channel model are shown in Fig. 1. The turbulence length scale was taken .014, channel bed, wall of the roughness were given wall boundary using no-slip boundary condition to set the velocity zero. The wall boundary condition requires specification of wall roughness parameters; roughness constant which we have specified as 0.5. FLUENT14 manual reports that choosing a roughness constant value of 0.5 when used with k – ε models, we have specified the roughness height .001 as per material property. In our present study we have kept the bed as net finished. For the air inlet boundary (Fig. 1), pressure inlet boundary was chosen and the turbulence intensity was specified as 0.001and air velocity was specified as 0.001 m/s. For the water inlet boundary (Fig. 1), pressure inlet boundary condition was chosen with and turbulence intensity was specified as 4.94% and velocity magnitude was specified as 0.2m/s, 0.3m/s depending on the run case. For the free surface (Fig. 1), symmetry boundary condition was chosen. But only one outlet was specified to let the solver decide the flow level at the outlet as calculated from inside the domain. For the outlet boundary, pressure outlet boundary condition was chosen and backflow turbulence was specified as 0, the bottom level was specified as 0m and free surface level as 0.4m. Using FLUENT14, the models were run using unsteady second order upwind implicit finite difference formulation. Convergence was achieved when the residuals of the mass continuity,$\overline{u_i}$ k, ε and α_w were 1/1000.

V. RESULTS AND DISCUSSION

In the outer layer the velocity profile deviates slightly from the log law, particularly in non-equilibrium boundary layers with a pressure gradient. Coles (1956) noted that the deviation or excess velocity above the log law had a wake-like shape relative to the free stream; i.e. $U = U_{\log law} + \Delta U\, f(y/\delta)$ Where f is some S-shaped function with f (0) = 0, f (1) = 1; $U_{\log law} = 1/\kappa^{*}\, ln\, y^{+} + B$; Where $\kappa^{*}$is the von Karman constant (κ^{*}=0.41), and B=5. For fully rough bed the transfer of momentum to the wall is predominantly by pressure drag on roughness elements, not viscous stresses, and wall friction becomes essentially independent of Reynolds number for sufficiently large Re. Dimensional analysis implies $U_{\log law} = 1/\kappa^{*}\, ln\, y/k_s + B_k$; where k_s is the roughness size.

A. Mean velocity profile

Considering u, v and w as the instantaneous stream-wise, lateral and vertical velocity components in the x, y and z direction respectively, and the following relation can be written $u = \bar{u} + u', v = \bar{v} + v'$, and $w = \bar{w} + w'$, where $\bar{u}, \bar{v}, \bar{w}$ are the mean time averaged velocity components and u', v', w' the corresponding instantaneous fluctuations. The mean velocities $\bar{u}$ at each measuring location were computed by standard procedure $\bar{u} = \frac{1}{n}\sum_{i=1}^{n} u_i$; where n is the total number of observations at each measuring location. From figure 2 we can see that the plot of stream wise mean velocity as a function of vertical distance (Z) for plane rigid bed at fully developed region (11.9m apart from the inlet) are in good agreement with the previous investigations (e.g., Nezu and Nakagawa 1993). By placing the roughness at 12m apart from the inlet, and measuring the stream wise velocity profile, the result was that the velocity increases in viscous sub layer as compared to that of plane bed. From the result we can notice that the velocity starts decreasing from z=0.15m. Further taking the velocity profile at 12.1m apart from inlet, a wake region is formed due to roughness, Due to the formation of wake region; the velocity is more not

only in the viscous sub layer but also in the logarithmic layer. From z=0.2m the velocity is decreasing up to the free surface layer as compared to the plane bed velocity profile.

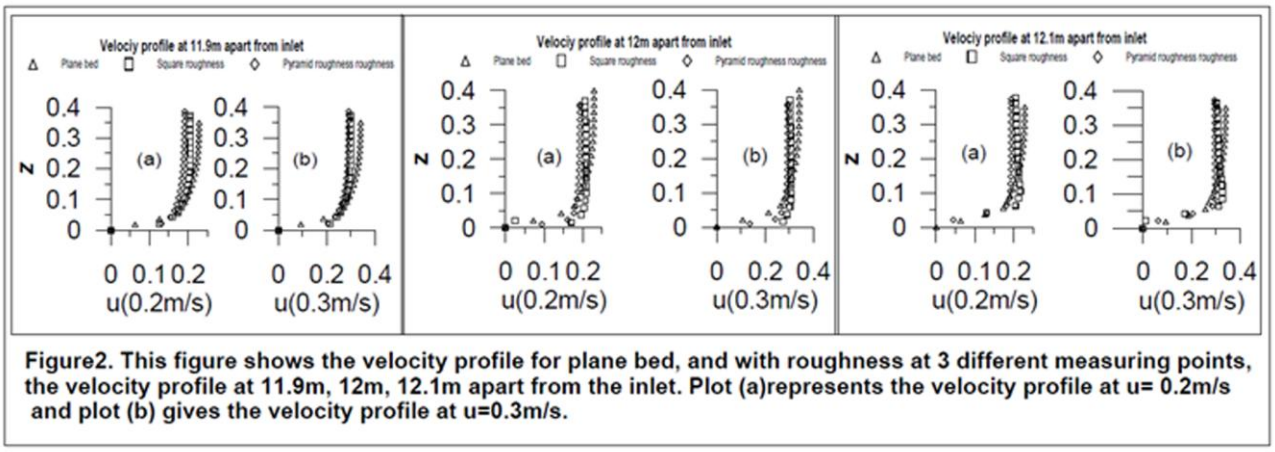

Figure2. This figure shows the velocity profile for plane bed, and with roughness at 3 different measuring points, the velocity profile at 11.9m, 12m, 12.1m apart from the inlet. Plot (a)represents the velocity profile at u= 0.2m/s and plot (b) gives the velocity profile at u=0.3m/s.

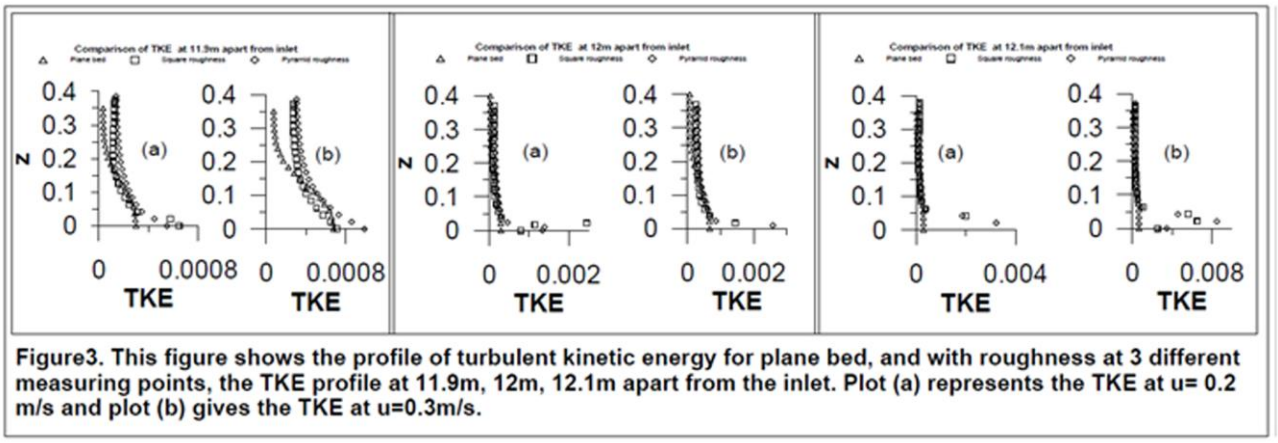

Figure3. This figure shows the profile of turbulent kinetic energy for plane bed, and with roughness at 3 different measuring points, the TKE profile at 11.9m, 12m, 12.1m apart from the inlet. Plot (a) represents the TKE at u= 0.2 m/s and plot (b) gives the TKE at u=0.3m/s.

B. Turbulent Kinetic Energy and Turbulent Intensity

On observing plot (a), we notice that the TKE profile of plane bed converges to zero as the vertical distance increases, but for the case of roughness, the TKE profile is slightly more than zero, and does not converge to zero as vertical distance increases. From z=0.2m the TKE profile of roughness is shifted as compared to that of plane bed. From plot(b) at comparison of TKE at 11.9m apart from inlet, we observed that the difference between the plane bed and roughness is more than that at u=0.2m/s, and the nature of TKE is same in both plane bed and roughness, however, the value of TKE is more for roughness. Plot (a) shows the profile of turbulent kinetic energy at 12m apart from inlet. The roughness is introduced from 12m apart from inlet, due to which the TKE increases in the viscous sub layer, however above z=0.1m the TKE remains zero for u=0.2m/s. Plot (b) of turbulent kinetic energy at 12m apart from inlet, shows the TKE profile for u=0.3m. The TKE profile follows the same trend as that of u=0.2m/s, however the TKE converges to zero above z=0.2m. Plot (a) of Fig (3) shows the profile of turbulent kinetic energy at 12.1m apart from inlet. The TKE increases more in the viscous sub layer due to wake region, however above z=0.1m the TKE remains zero for u=0.2m/s. Plot (b) of turbulent kinetic energy at 12m apart from inlet, shows the TKE profile for u=0.3m. The TKE profile follows the same trend as that of u=0.2m/s, however the TKE converges to zero above z=0.1m.

C. Turbulent intensity (u^+)

On observing the plane bed profile at plot(a), TI is converging to zero at z=0.35m for the case of 11.9m apart from inlet, whereas for the case of 12m and 12.1m apart from inlet, the TI profile for plane bed does not converge to zero. On observing the roughness profile, the TI increases from z=0.2m for the case of 11.9m apart from inlet, however for the case of 12m and 12.1m apart from inlet, the TI is more in viscous sub layer region, and tracks the same trend as TI of plane bed condition. Plot (b) shows the TI profile u=0.3m/s. On observing the TI for the three cases i.e. 11.9m, 12m and 12.1m apart from inlet, the TI of plane bed does not converge to zero for 11.9m apart from inlet, on contradict to the TI profile of plane bed at u=0.2m, whereas rest of the TI profile are same as that of plot (a) for u=0.2m.

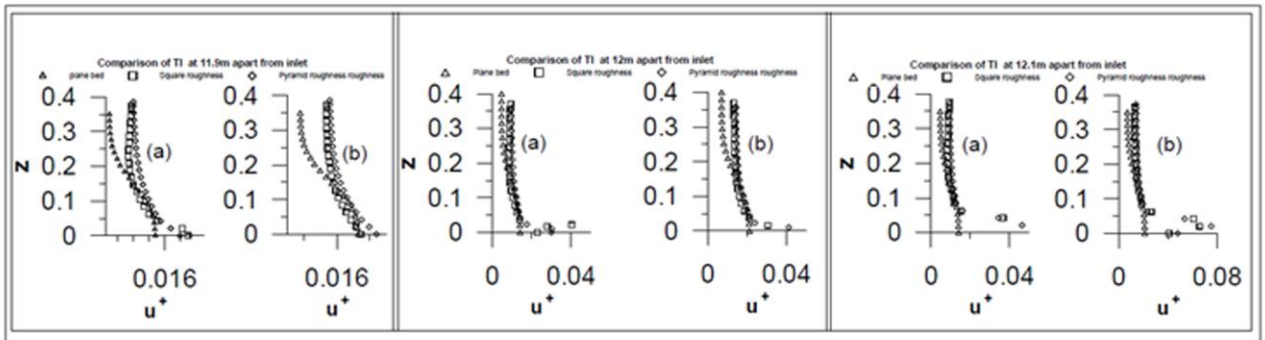

Figure4. This figure represents the turbulent intensity for plane bed and roughness. Plot (a) shows the turbulent intensity profile for u=0.2m/s. The turbulent intensity has been studied at 11.9m apart from inlet, at 12m apart from inlet introducing roughness, and at 12.1m apart from inlet at wake region.

VI. CONCLUSIONS

VOF model of open channels has been developed using FLUENT14 for different velocities and roughness. Effect of longitudinal and vertical velocity, turbulence kinetic energy, dissipation on changes in relative roughness is tested for two different Reynolds number. The present model results have been validated with results of Nezu and Nakagawa (1993) and provided reasonably conformity. It has been observed that for roughness shape variation results in more significant change in flow structure Compared to changes in Reynolds number. It can be seen that with changes of roughness shape, longitudinal velocity in general decreases but increase after roughness at the viscous sub layer. Three distinct zones can be observed in the Velocity profiles with the middle zone resembling a zone of strong mixing. Longitudinal velocity profile resemble a mixing layer velocity profile and an inflection point occurs at a point z=0.15. With roughness shape variation TKE Increase up to at 0.2 - 0.4z,. After roughness TKE is decreases but it increases at viscous sub layer. With increase in flow Reynolds number the phenomenon remains same. the free surface vertical velocity component shows a region of strong gradient in the central region that resembles that of a mixing layer instead of a shear layer as mostly concluded in the case of studies with terrestrial roughness.

REFERENCES

[1] Leonardi, S., P. Orlandi, R. J.Smalley, L. Djenidi, and R.A. Antonia, Direct numerical simulations of turbulent channel flow with transverse square bars on one wall, J. Fluid Mech. 491, 229-238. 2003.

[2] Stoesser, T., Matthey, F., Fröhlich, J., Rodi W., LES of Flow over Multiple Cubes. ERCOFTAC Bulletin No. 56: Complex Flow Problems.2003.

[3] Jiménez, J., Turbulent Flows Over Rough Walls. Annu. Rev. Fluid Mech., 36, 173–96. 2004.

[4] Bailon-Cubaa, J., Brzeka B., L. Stefano and C. Luciano, Theoretical evaluation of the Reynolds shear stress and flowparameters in transitionally rough turbulent boundary Layers, Journal of Turbulence. Vol. 10, No. 5, 1–28. 2009.

[5] Stoesser, T., V. Nikora, Flow structure over square bars at intermediate submergence: Large Eddy Simulation study of bar spacing effect, Acta Geophysica Volume 56, Issue 3, pp 876-893. 2008.

[6] Keshmiri, A., Numerical sensitivity analysis of 3- and 2- dimensional rib-roughened channels, Heat Mass Transfer doi 10.1007/s00231-012-0968-z. 2012.

[7] Nezu, I., Nakagawa, H., Turbulence in open-channel flows. IAHR Monograph Series. Rotterdam: A.A.Balkema. 1993.

[8] Nikora, V., D. Goring, I. McEwan, and G. Griffiths, Spatially-averaged open-channel flow over a rough bed, J. Hydraul. Eng. ASCE 127, 123-133. 2001.

[9] Nikora, V., K. Koll, I. McEwan, S. McLean, and A. Dittrich, Velocity distribution in the roughness layer of rough-bed flows, J. Hydraul. Eng, ASCE 130, 1036-1042. 2004.

[10] Nikora, V., I. McEwan, S. McLean, S. Coleman, D. Pokrajac, and R. Walters, Double-averaging concept for rough-bed open-channel and overland flows: Theoretical background, J. Hydraul. Eng. ASCE 133, 873-883. 2007a.

[11] Nikora, V., I. McEwan, S. McLean, S. Coleman, D. Pokrajac, J. Aberle, L. Campbell, K. Koll, and T.M. Clunie, Double-averaging concept for rough-bed open-channel and overland flows: Applications, J. Hydraul. Eng. ASCE 133, 884-895. 2007b.

[12] Perry, A.E., W.H. Schofield, and P.N. Joubert, Rough wall turbulent boundary layers, J. Fluid Mech. 37, 2, 383-413. 1969.

[13] Perry, A.E., K.L. Lim, and S.M. Henbest, An experimental study of the turbulence structure in

smooth- and rough-wall boundary layers, J. Fluid Mech. 177, 437-466. 1987.

[14] Polatel, C., Large-scale roughness effect on free-surface and bulk flow characteristics in open-channel flows, Ph.D. Thesis, Iowa Institute of HydraulicResearch, The University of Iowa. 2006.

[15] Raupach, M.R., R.A. Antonia, and S. Rajagopalan, Rough-wall turbulent boundary layers, Appl. Mech. Rev. ASME 44, 1-25.

[16] Stoesser, T. (2002), Development and validation of a CFD code for open-channe flows, PhD Thesis, Department of Civil Engineering, Bristol University. 1991.

[17] Stoesser, T., and W. Rodi, LES of bar and rod roughened channel flow, Proc. Sixth Int. Conf. on Hydro-Science and Engineering, Brisbane, Australia (CD ROM, 12 p). 2004.

[18] Townsend, A.A., The Structure of Turbulent Shear Flow, Cambridge University Press, Cambridge, 2nd ed., 429 pp. 1976.

[19] Yaglom, A.M., Similarity laws for constant-pressure and pressure-gradient turbulent wall flows, Ann. Rev. Fluid Mech. 11, 505-540. 1979.